Supplementary Information

Compressed carbon nanotubes: A family of new multifunctional carbon allotropes

Meng Hu,[1†] Zhisheng Zhao,[1†‡] Fei Tian,[2†] Artem R. Oganov,[3] Qianqian Wang,[1] Mei Xiong,[1] Changzeng Fan,[1] Bin Wen,[1] Julong He,[1] Dongli Yu,[1] Hui-Tian Wang,[2] Bo Xu,[1*] & Yongjun Tian[1*]

[1]State Key Laboratory of Metastable Materials Science and Technology, Yanshan University, Qinhuangdao 066004, China, [2]School of Physics and Key Laboratory of Weak-Light Nonlinear Photonics, Ministry of Education, Nankai University, Tianjin 300071, China, [3]Department of Geosciences, and Department of Physics and Astronomy, Stony Brook University, Stony Brook 11794-2100, NY, USA

[‡] Current address: High Pressure Collaborative Access Team, Geophysical Laboratory, Carnegie Institution of Washington, Argonne, Illinois 60439, USA.

[*] Correspondence and requests for materials should be addressed to B.X. (bxu@ysu.edu.cn) and Y.J.T. (fhcl@ysu.edu.cn)

[†] These authors contributed equally to this work.

Contents

Computation details

Constructing of carbon nanotube bundles Nanotube bundle building process in Materials Studio can be logically separated in two parts[1]: determining the positions of the atoms and establishing the bonding pattern in the nanotube. Atomic positions are defined unambiguously by the chiral vector and by the bond length of an ideal graphene sheet. The actual bonds are created between nanotube atoms based on the setting of the connectivity option for bond calculations.

Applying pressure The "pressure" is applied by CASTEP code[1]. The methodology in CASTEP is very similar to the real experiment: the structure is full relaxed under fixed external pressure. The relaxation is successful until the internal stress of the structure is equal to the applied external pressure. To guarantee the compressed structure can be achieved in the ambient pressure, we further relax it without external pressure. Then the quenched structure is used to investigate its electronic and mechanical properties.

Band structure, elastic constants, and bulk and shear modulus Band structures were calculated along the high symmetrical k points of Brillouin Zone, and primitive cell were used. Considering density functional theory (DFT) can systematically underestimate the band gaps by about 30%-40%, the semiconducting nanotube polymers would have larger band gaps. Elastic constants C_{ij} are calculated using primitive cell. After applying a finite strain to the optimized structure, the elastic constants can be determined from the linear relationship (Hooke's law) between the applied strain and the resulting stress. For each distorted structure, the atomic coordinates were optimized with fixed lattice parameters in order to obtain the internal stress of crystal. The bulk and shear modulus were calculated according to the Voigt-Reuss-Hill rule.

Hardness The Vickers hardness of the 3D polymers is calculated based on our semi-empirical model[2-5]. For semiconducting and metallic carbons, the formulae are $H_v = 350 N_e^{2/3} e^{-1.191 f_i} / d^{2.5}$ and $H_v = 350 N_e^{2/3} e^{-1.191 f_i - 32.2 f_m^{0.55}} / d^{2.5}$, respectively. N_e is the valence electron density, evaluated as $N_e = n_c Z_c / V$, whereas n_c is the number of carbon atoms in the unit cell, Z_c is the valence electron number of atoms which is 4 for carbon, and V is the volume of a unit cell. f_i is the Phillips ionicity of the C−C bond, which is equal to 0. f_m is a factor of metallicity, calculated by $f_m = 0.026 D_F / n_e$, with D_F being the total density of states (DOS) of a unit cell at the Fermi level, and n_e being the total number of valence electrons in the unit cell. d is the average C−C bond length, calculated using $d = \sum_j N^j d^j \Big/ \sum_j N^j$, with N^j being the number of the j bond in the unit cell, and d^j being the j bond length. This model has been successfully applied on calculating the hardness of cubic diamond[2].

Tensile strength We previously proposed an microscopically model to evaluate the tensile strength of a crystal in specified [*hkl*] direction[6]. According to the model, the ideal tensile strength in a specified direction is determined by the bond strength and broken bond number via $\sigma_{hkl}^{theor}(Pa) = F_{ij} S_{hkl}$, where F_{ij} is the bond strength and S_{hkl} is the number of the broken bonds per unit area on the (*hkl*) plane, which has the lowest bond density. The bond strength of *i-j* bond is proposed to be equal to the maximum tensile force F_{ij} unbinding *i-j* bond, and proven to be exclusively dependent on two microscopic parameters: bond length d_{ij} and effectively bonded valence electron (EBVE) number n_{ij}. Here n_{ij} is calculated from $n_{ij} = n_i n_j \Big/ \sqrt{n_i^2 + n_j^2}$ with $n_i = Z_i / N_i$ and $n_j = Z_j / N_j$, where Z_i and Z_j are the valence electron numbers of atom *i* and *j*, respectively (for carbon, they are both 4); and N_i and N_j are the coordination numbers of atoms *i* and *j*, respectively. F_{ij} is calculated as $F_{ij}(N) = 6.6 \times 10^{-10} d_{ij}^{-1.32} \exp(3.7 n_{ij})$. The calculated tensile strength based on our model of graphene in the zigzag <10> direction and (10, 0) nanotubes in the axial direction are 162.7 and 161.0 GPa, respectively, which are in excellent agreement with recent reports[6]. Tensile strengths for the carbon nanotube polymers along the radial and axial directions are calculated (Table 1, Table S3, and Table S4).

Mechanical properties

Tensile Strength The experimental tensile strength of defect-free graphene and carbon nanotubes can reach 130 ± 10 and 150 ± 45 GPa, respectively[7,8]. Here, the theoretical tensile strengths in radial and axial directions are microscopically determined (Table S3 and S4). In the axial directions, 3D (6,0)-IV takes the lowest tensile strength of 34.5 GPa, whereas the 3D-(4,0)-II carbon has the highest strength of 210.0 GPa for the fairly short bonds. The others are all take the values >75 GPa. Obviously, the high axial tensile strength is preserved in the polymers. In the radial direction, the 3D (4,0)-II carbon has the lowest tensile strength of 22.2 GPa, whereas the 3D-(2,2)-II carbon has the highest strength of 112.9 GPa, approaching to the experimental values of graphene and carbon nanotubes.

Young's modulus 1D carbon nanotubes are highly stiff in the axial directions. Theoretical and experimental results demonstrate that the axial Young's modulus are insensitive to the radius and chirality, and the values are around 1 TPa, which are consistent with the in-plane isotropic Young's modulus of a graphene sheet[9,10]. However, the radial direction is flexible and elastic. The experimentally obtained radial moduli of multi-walled nanotubes are only 0.3-4.0 GPa and 9.7-80.0 GPa[11,12]. 3D polymers inherit the high Young's modulus of the parent SWCNTs along the axial direction with values around 1 TPa

(Table 1). The radial Young's modulus are improved to higher than 100 GPa, and the 3D (2,2)-III have the highest modulus at TPa magnitude.

Ductility/brittleness Diamond is the hardest material in the world, but it is rather brittle, which limits its industry application. The ductility/brittleness can be qualitative evaluated by Poisson's ratio and the ratio of bulk modulus (B) to shear modulus (G) (Table 1). Paugh[13] proposed that a high (low) B/G value is often associated with ductility (brittleness) and the critical value to differentiate ductile from brittle for a material is about 1.75. 3D (6,0)-IV have the smallest B/G radio of 0.83, which is equal to that of diamond (0.83). All the others show better ductility than diamond with higher B/G radio. The B/G of 3D (6,0)-II is 1.76, illustrating its ductile nature. For conviction, the brittleness/ductility character is further evaluated by Frantsevich rule employing Poisson's ratio[14]: a high (low) Poisson's ratio value usually suggests ductility (brittleness) with a critical value of 1/3. This rule gives the consistent brittleness/ductility results, *i.e.* 3D (6,0)-IV is as brittle as diamond with the same Poisson's ratio of 0.07, and all the others are more ductile than diamond.

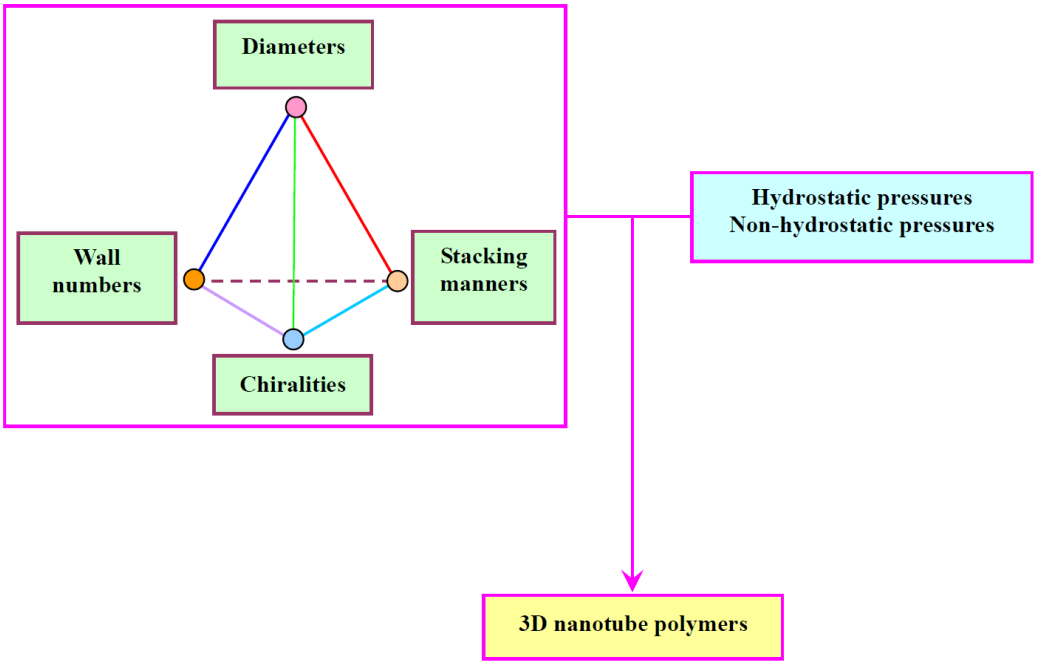

Figure S1 | Schematic diagram for designing novel 3D nanotube polymers. The left framework is related to the raw carbon nanotubes with different diameters, chiralities, stacking manners, and wall numbers. The four factors comprise a tetrahedron. The point, line, face, and the whole tetrahedron represent different factor assemblies, which yield various raw CNT materials.

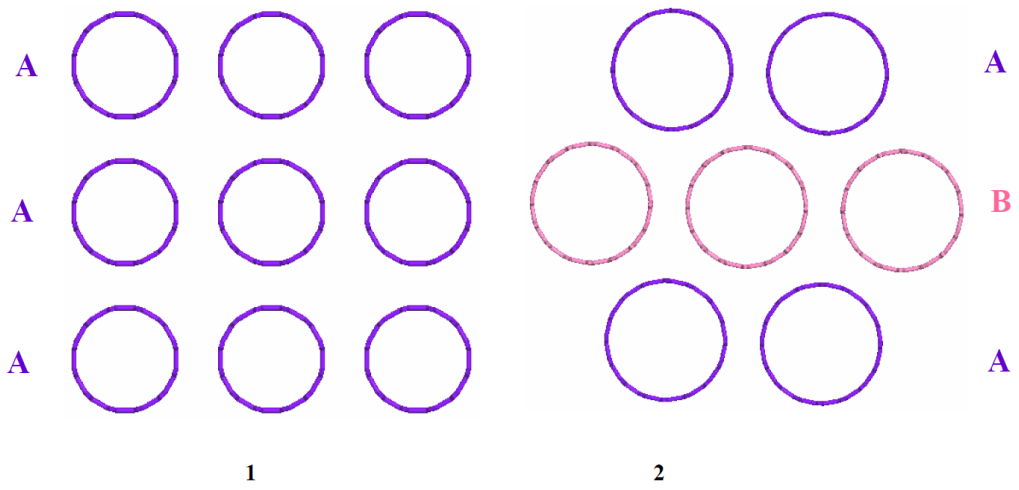

Figure S2 | Stacking manner of SWCNTs. The pink (A) and purple (B) circles represent the identical nanotubes but distinct positioning.

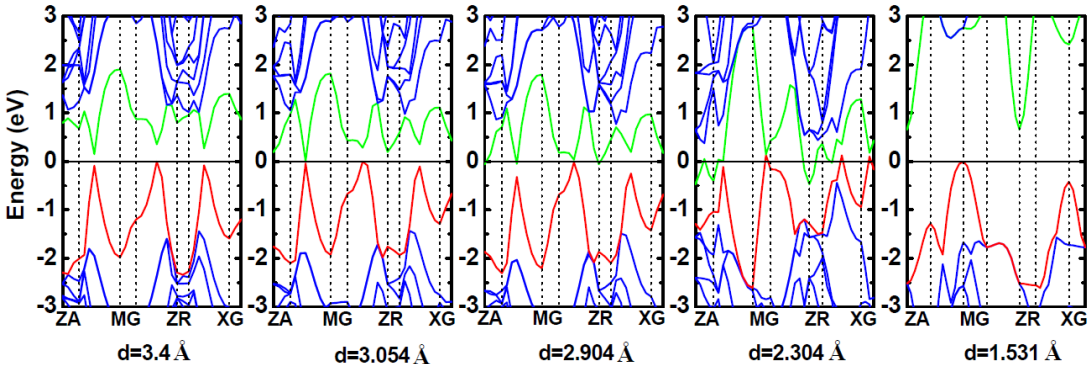

Figure S3 | Band structures at different intertube distances, d (Å), in the transition from aligned (4,4) SWCNTs to 3D (4,4) carbon at 35 GPa.

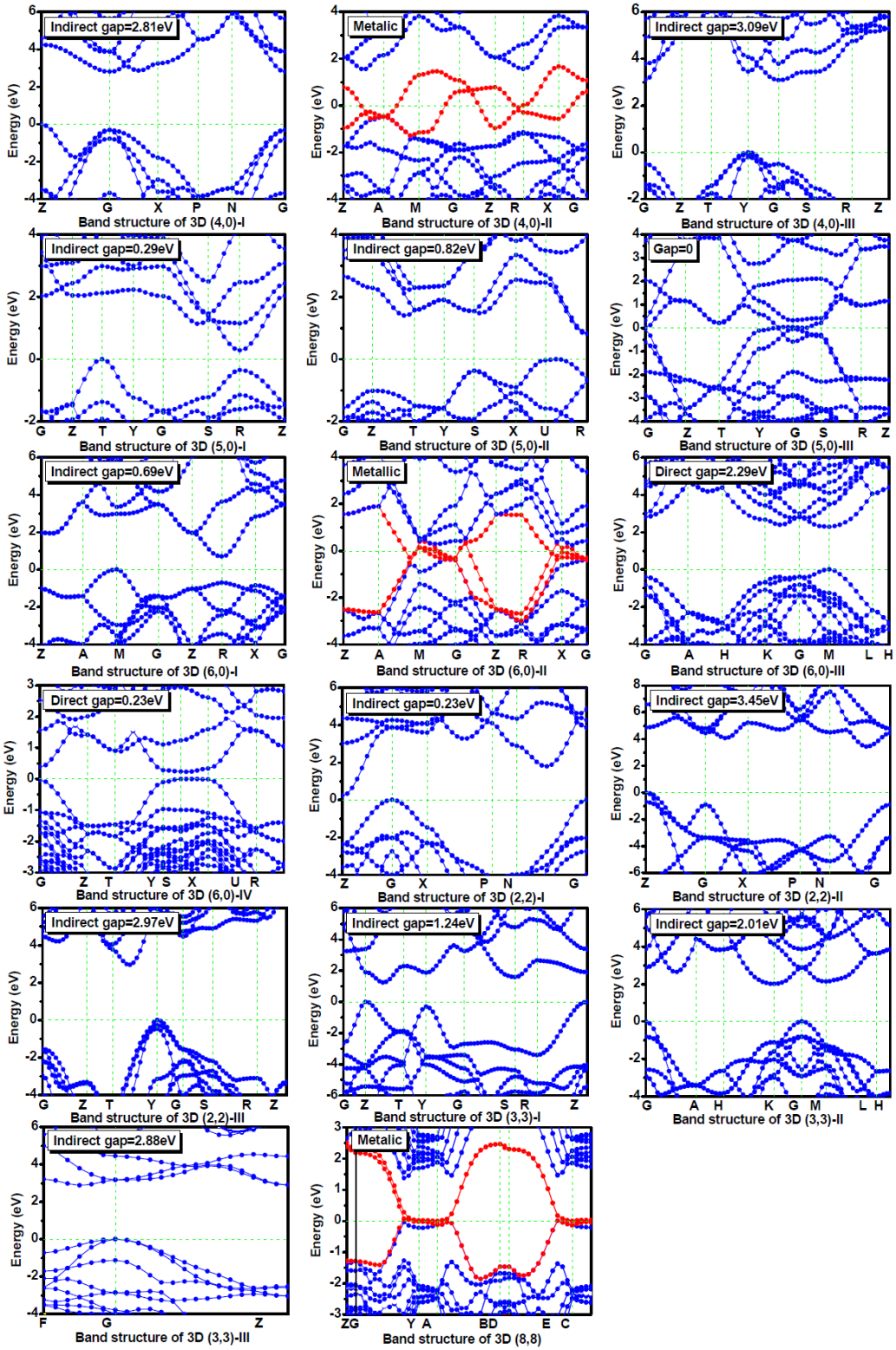

Figure S4 | Electronic band structures of 3D (*n*,0) and 3D (*n*,*n*) carbons at ambient pressure. The red lines represent the bands crossing through the Fermi levels.

Table S1 | Space group (S.G.), cell parameters (Å), and atomic Wyckoff positions of carbon allotropes at ambient pressure.

Structure	S.G.	*a*	*b*	*c*	*β*	Atomic positions
3D (4,0)-I	*I*4/*mcm* (140)	4.882		4.145		16*l* (0.850, 0.650, 0.185)
3D (4,0)-II	*P*4/*mmm* (123)	5.249		4.206		8*t* (1/2, 0.849, 0.182); 8*r* (0.277, 0.723, 0.339)
3D (4,0)-III	*Cccm* (66)	10.073	4.482	4.217		16*m* (0.816, 0.344, 1.182); 16*m* (0.928, 0.162, 1.314)
3D (5,0)-I	*Cmmm* (65)	12.160	4.247	5.806		16*r* (0.384, 0.342, 0.706); 16*r* (0.810, 0.321, 0.864); 8*q* (0.434, 0.819, 1/2)
3D (5,0)-II	*Pmma* (51)	4.204	5.810	6.054		8*l* (0.910, 0.295, 0.769); 8*l* (0.929, 0.136, 0.379); 4*j* (0.566, 1/2, 0.125)
3D (5,0)-III	*Cmcm* (63)	7.368	9.778	4.172		4*f* (0.660, 0.085, 0.780); 4*f* (0.780, 0.585, 0.660); 4*f* (0.876, 0.066, 0.481); 4*f* (0.730, 0.588, 0.270); 4*f* (0.519, 0.066, 0.124)
3D (6,0)-I	*P*42/*mmc* (131)	4.729		4.139		4*i* (0, 1/2, 0.337); 8*p* (0.723, 1/2, 0.817)
3D (6,0)-II	*P*42/*mmc* (131)	6.925		4.263		16*r* (0.787, 0.667, 0.337); 8*p* (0.886, 1/2, 0.819)
3D (6,0)-III	*P*6/*mcc* (192)	6.817		4.090		24*m* (0.452, 0.329, 0.185)
3D (6,0)-IV	*Pccm* (49)	7.302	11.501	4.200		8*r* (0.606, 0.567, 0.316); 8*r* (0.750, 0.642, 0.839); 8*r* (0.892, 0.718, 0.316); 8*r* (0.418, 0.890, 0.338); 8*r* (0.243, 0.933, 0.816); 8*r* (0.098, 0.850, 0.315)
3D (2,2)-I	*I*4/*mmm* (139)	6.463		2.475		16*l* (0.115, 0.713, 1/2)
3D (2,2)-II	*I*4/*mmm* (139)	4.329 4.322[a]		2.483 2.478[a]		8*h* (0.344, 0.344, 0)
3D (2,2)-III	*Cmmm* (65)	8.674[b]	4.209[b]	2.487[b]		8*q* (-0.170, 0.815, 1/2); 8*p* (-0.089, 0.315, 0)
3D (3,3)-I	*Cmmm* (65)	6.071[c]	2.482[c]	5.201[c]		4*k* (1/2, 1/2, 0.872); 4*h* (0.681, 0, 1/2); 4*l* (1/2, 0, 0.282)
3D (3,3)-II	*P*63/*mmc* (194)	6.055		2.518		12*j* (0.408, 0.082, 1/4)
3D (3,3)-III	*R*-3*m* (166)	10.394[d]		2.467[d]		36*i* (0.048, 0.244, 0.262)

3D (8,8)	*P*2/*m* (10)	8.938	2.482	18.775	111.40	2*m* (0.978, 0, 1.054); 2*m* (0.864, 0, 0.966); 2*m* (0.986, 0, 0.786); 2*m* (0.786, 0, 0.541); 2*m* (0.924, 0, 0.704); 2*m* (0.713, 0, 0.459); 2*m* (0.575, 0, 0.297); 2*m* (0.478, 0, 0.055); 2*m* (0.514, 0, 0.214); 2*m* (0.364, 0, -0.034); 2*n* (0.760, 1/2, 0.959); 2*n* (0.928, 1/2, 1.088); 2*n* (1.014, 1/2, 0.826); 2*n* (0.892, 1/2, 0.663); 2*n* (0.677, 1/2, 0.419); 2*n* (0.823, 1/2, 0.581); 2*n* (0.607, 1/2, 0.337); 2*n* (0.486, 1/2, 0.174); 2*n* (0.260, 1/2, -0.041); 2*n* (0.428, 1/2, 0.088)

a Ref. [15], b Ref. [16], c Ref. [17], d Ref. [18].

Tabel S2 | Bond parameters and Vickers hardness of 3D (*n*,0) and 3D (*n*,*n*) carbons. V (Å^3) is the volume of the unit cell, d (Å) is the average bond length, n is the bond number in unit cell, N_e (Å^{-3}) is the valence electron density, f_m is the bond metallicity, and $H_{v\text{calc}}$ (GPa) is the calculated Vickers hardness, respectively.

Structure	V	d	n	N_e	f_m ($\times 10^{-3}$)	$H_{v\text{calc}}$
3D (4,0)-I	98.81	1.53	32	0.65	0	89.9
3D (4,0)-II	115.88	1.49	28	0.55	0.69	47.9
3D (4,0)-III	190.42	1.54	64	0.67	0	91.9
3D (5,0)-I	299.85	1.50	72	0.53	0	83.2
3D (5,0)-II	147.88	1.50	34	0.54	0	84.5
3D (5,0)-III	300.43	1.50	56	0.53	0	83.4
3D (6,0)-I	92.57	1.51	22	0.52	0	81.07
3D (6,0)-II	204.42	1.46	36	0.47	0.82	43.0
3D (6,0)-III	164.60	1.54	48	0.58	0	83.7
3D (6,0)-IV	352.72	1.53	88	0.54	0	80.1
3D (2,2)-I	103.41	1.53	32	0.62	0	88.1
3D (2,2)-II	46.53	1.53	16	0.69	0	93.6
3D (2,2)-III	90.8	1.53	32	0.70	0	95.2
3D (3,3)-I	78.37	1.50	22	0.61	0	90.9
3D (3,3)-II	79.94	1.53	24	0.60	0	85.5
3D (3,3)-III	230.82	1.55	72	0.62	0	85.3

Tabel S3 | Axial tensile strength σ_a (GPa) of 3D (n,0) and 3D (n,n) carbons. Bond length d_{ij} (Å); effectively bonded valence electron (EBVE) number n_{ij}; S_{hkl} (m^{-2}) is the number of the broken bonds per unit area on the (hkl) plane, which has the lowest bond density; and the maximum tensile force F_{ij} (nN) unbinding i-j bond.

Structure	d_{ij}	n_{ij}	S_{hkl} ($\times 10^{20}$)	F_{ij}	σ	σ_{total}
3D (4,0)-I	1.54	0.707	0.17	5.12	85.95	86.0
3D (4,0)-II	1.36	0.943	0.15	14.47	210.03	210.0
3D (4,0)-III	1.57	0.707	0.09	5.00	44.27	89.8
	1.53	0.707	0.09	5.14	45.53	
3D (5,0)-I	1.54	0.707	0.03	5.11	14.48	127.1
	1.52	0.707	0.06	5.22	29.55	
	1.34	0.943	0.06	14.66	83.07	
3D (5,0)-II	1.54	0.707	0.03	5.09	14.49	127.7
	1.50	0.707	0.06	5.27	29.97	
	1.34	0.943	0.06	14.65	83.29	
3D (5,0)-III	1.53	0.707	0.06	5.13	28.52	147.4
	1.38	0.943	0.06	14.15	78.56	
	1.35	0.707	0.03	14.52	40.32	
3D (6,0)-I	1.35	0.943	0.04	14.62	65.37	112.2
	1.51	0.707	0.09	5.23	46.80	
3D (6,0)-II	1.39	0.943	0.08	13.96	116.42	137.7
	1.54	0.707	0.04	5.10	21.29	
3D (6,0)-III	1.52	0.707	0.15	5.22	77.75	77.8
3D (6,0)-IV	1.36	0.943	0.02	14.48	34.48	34.5
3D (2,2)-I	1.52	0.707	0.19	5.18	99.19	99.2
3D (2,2)-II	1.69	0.707	0.21	4.51	96.27	96.3
3D (2,2)-III	1.53	0.707	0.22	5.16	113.00	113.0
3D (3,3)-I	1.48	0.800	0.13	7.61	96.42	130.0
	1.50	0.707	0.06	5.30	33.59	129.98[a]
3D (3,3)-II	1.52	0.707	0.19	5.18	97.87	97.9
3D (3,3)-III	1.56	0.707	0.13	5.04	64.68	99.9
	1.46	00.707	0.06	5.49	35.21	76.5[b]

a Ref. [18]
b Ref. [19]

Tabel S4 | Radial tensile strength σ_r (GPa) of 3D (n,0) and 3D (n,n) carbons. Bond length d_{ij} (Å); effective bonded valence electron (EBVE) number n_{ij}; S_{hkl} (m^{-2}) is the number of the broken bonds per unit area on the (hkl) plane, which has the lowest bond density; and the maximum tensile force F_{ij} (nN) unbinding i–j bond.

Structure	d_{ij}	n_{ij}	S_{hkl} ($\times 10^{20}$)	F_{ij}	σ	σ_{total}
3D (4,0)-I	1.48	0.707	0.14	5.36	74.99	75.0
3D (4,0)-II	1.59	0.707	0.05	4.90	22.18	22.2
3D (4,0)-III	1.51	0.707	0.09	5.23	49.24	97.0
	1.55	0.707	0.09	5.07	47.73	
3D (5,0)-I	1.58	0.707	0.08	4.94	38.25	38.3
3D (5,0)-II	1.62	0.707	0.08	4.80	39.28	39.3
3D (5,0)-III	1.57	0.707	0.10	4.99	48.96	49.0
3D (6,0)-I	1.59	0.707	0.14	4.88	70.54	70.5
3D (6,0)-II	1.58	0.943	0.07	11.80	79.94	79.9
3D (6,0)-III	1.55	0.707	0.14	5.06	72.60	72.6
3D (6,0)-IV	1.41	0.800	0.05	8.08	38.47	60.7
	1.65	0.707	0.05	4.67	22.23	
3D (2,2)-I	1.49	0.707	0.13	5.32	66.53	66.5
3D (2,2)-II	1.35	0.707	0.19	6.07	112.86	112.9
3D (2,2)-III	1.56	0.707	0.09	5.03	93.4	93.4
3D (3,3)-I	1.58	0.707	0.15	4.94	76.57	76.6 76.5[a]
3D (3,3)-II	1.48	0.707	0.05	5.38	28.81	54.7
	1.61	0.707	0.05	4.83	25.85	
3D (3,3)-III	1.54	0.707	0.14	5.11	69.09	69.1 118.6[b]

a Ref. [18]
b Ref. [19]

Tabel S5 | Elastic constants C_{ij} (GPa), bulk modulus B (GPa), and shear modulus G (GPa) of 3D (n,0) and 3D (n,n) carbons. Gaphite, diamond and SWCNTs are also listed for comparison.

Structure	C_{11}	C_{22}	C_{33}	C_{44}	C_{55}	C_{66}	C_{12}	C_{13}	C_{16}	C_{23}	B	G
Graphite	1052.2		17.1	0.3 0.25-1.2[a]			194.9	-6.1			16.3 14.0-16.9[b]	0.6 0.25-1.2
Diamond	1092.9			595.4			135.4				456.6 442[c]	542.6 544[c]
3D (4,0)-I	742.0		1251.7	399.1		463.6	368.9	14.2	0		391.5	379.9
3D (4,0)-II	448.4		927.1	224.9		100.0	179.9	71.7	0		267.5	190.5
3D (4,0)-III	963.6	897.4	1101.2	404.0	359.2	456.2	201.8	69.4		43.5	398.7	416.3
3D (5,0)-I	360.0	892.6	459.5	324.3	238.3	208.7	82.9	263.1		112.0	283.1	204.8
3D (5,0)-II	933.3	467.1	376.3	250.5	262.3	326.5	93.1	60.2		273.0	284.2	220.3
3D (5,0)-III	438.0	613.1	1006.0	310.2	223.6	61.6	114.5	27.6		69.4	264.1	200.3
3D (6,0)-I	730.8		1032.9	305.2		56.7	25.6	45.3	0		298.6	231.1
3D (6,0)-II	280.4		855.3	188.0		155.7	226.8	76.0	0		231.1	131.0
3D (6,0)-III	746.3		1194.7	334.1			142.8	16.7			334.14	352.81
3D (6,0)-IV	563.9	305.7	928.7	251.6	347.7	246.4	154.3	-14.8		-21.4	212.6	257.2
3D (2,2)-I	864.8		1047.6	347.4		110.3	231.6	24.8	0		371.1	289.2
3D (2,2)-II	969.2		1240.4	465.9		316.0	172.5	55.9	0		415.6	434.2
3D (2,2)-III	1113.1	1153.4	1226.5	470.1	525.2	366.2	68.9	87.8		22.3	427.7	487.1
3D (3,3)-I	509.9	1145.8	1031.7	455.8	126.1	229.2	39.5	152.7		108.5	343.9	283.6
3D (3,3)-II	775.5		949.7	314.8			184.9	60.4			345.6	324.3
3D (3,3)-III	766.0		1128.7	350.7			213.9	31.6			356.04	345.09
(4,0)	0.94		664.1	12.2		4.7	-13.4	3.6	0.4		33.1	30.7
(6,0)	12.3		822.7				0.5	-7.1			16.2	11.8
(8,0)	13.6	11.1	806.7	65.9	85.9	8.1	-2.3	-5.7		-5.3	14.8	14.1
(2,2)	52.7		880.4	4.4		12.4	3.1	6.9	0		70.4	38.6
(4,4)	30.2	21.9	852.1	24.6	24.9	15.0	9.4	-6.2		-5.1	16.6	24.3
(6,6)	20.2		749.0	22.3			10.0	-5.1			14.6 41.7[d], 15-33[e]	9.9 0.7-6.5 (±50%)[f]

a Experimental value, Ref. [19]
b Experimental value, Ref. [20]
c Experimental value, Ref. [21]
d Experimental value of single-walled carbon nanotubes bundles, Ref. [22]
e Calculated value of crystalline nanoropes composed of single-walled carbon nanobutes, Ref. [23]
f Experimental value, Ref. [24]

Reference

1 Clark, S. J. *et al.* First principles methods using CASTEP. *Zeitschrift für Kristallographie* **220**, 567-570 (2005).

2 Gao, F. *et al.* Hardness of Covalent Crystals. *Phys. Rev. Lett.* **91**, 015502 (2003).

3 He, J., Wu, E., Wang, H., Liu, R. & Tian, Y. Ionicities of Boron-Boron Bonds in B_{12} Icosahedra. *Phys. Rev. Lett.* **94**, 015504 (2005).

4 Guo, X. *et al.* Hardness of covalent compounds: Roles of metallic component and d valence electrons. *J. Appl. Phys.* **104**, 023503 (2008).

5 Tian, Y., Xu, B. & Zhao, Z. Microscopic theory of hardness and design of novel superhard crystals. *Int. J. Refract. Met. Hard Mater.* **33**, 93-106 (2012).

6 Guo, X. *et al.* Unbinding force of chemical bonds and tensile strength in strong crystals. *J. Phys.: Condens. Matter* **21**, 485405 (2009).

7 Lee, C., Wei, X., Kysar, J. W. & Hone, J. Measurement of the Elastic Properties and Intrinsic Strength of Monolayer Graphene. *Science* **321**, 385-388 (2008).

8 Demczyk, B. *et al.* Direct mechanical measurement of the tensile strength and elastic modulus of multiwalled carbon nanotubes. *Mater. Sci. Eng., A* **334**, 173-178 (2002).

9 Wong, E. W., Sheehan, P. E. & Lieber, C. M. Nanobeam Mechanics: Elasticity, Strength, and Toughness of Nanorods and Nanotubes. *Science* **277**, 1971-1975 (1997).

10 Treacy, M. M. J., Ebbesen, T. W. & Gibson, J. M. Exceptionally high Young's modulus observed for individual carbon nanotubes. *Nature* **381**, 678-680 (1996).

11 Yu, M.-F., Kowalewski, T. & Ruoff, R. S. Investigation of the Radial Deformability of Individual Carbon Nanotubes under Controlled Indentation Force. *Phys. Rev. Lett.* **85**, 1456-1459 (2000).

12 Shen, W., Jiang, B., Han, B. S. & Xie, S.-s. Investigation of the Radial Compression of Carbon Nanotubes with a Scanning Probe Microscope. *Phys. Rev. Lett.* **84**, 3634-3637 (2000).

13 Pugh, S. F. XCII. Relations between the elastic moduli and the plastic properties of polycrystalline pure metals. *Phil. Mag.* **45**, 823-843 (1954).

14 Frantsevich, I., Voronov, F. & Bokuta, S. Elastic constants and elastic moduli of metals and insulators handbook. *Naukova Dumka, Kiev*, 60-180 (1983).

15 Zhou, X.-F. *et al.* Ab initio study of the formation of transparent carbon under pressure. *Phys. Rev. B* **82**, 134126 (2010).

16 Zhao, Z. *et al.* Novel Superhard Carbon: C-Centered Orthorhombic C_8. *Phys. Rev. Lett.* **107**, 215502 (2011).

17 Zhao, Z. *et al.* Three Dimensional Carbon-Nanotube Polymers. *ACS Nano* **5**, 7226-7234 (2011).

18 He, J., Zhao, Z. & Tian, Y. New three-dimensional (3,3) carbon nanotube polymer. *Journal of Yanshan University* **35**, 471-475 (2011).

19 Grimsditch, M. Shear elastic modulus of graphite. *Journal of Physics C: Solid State Physics* **16**, L143 (1983).

20 *http://www.phy.mtu.edu/~jaszczak/graphprop.html*.

21 Brazhkin, V. V., Lyapin, A. G. & Hemley, R. J. Harder than diamond: Dreams and reality. *Philos. Mag. A* **82**, 231-253 (2002).

22 Tang, J. *et al.* Compressibility and Polygonization of Single-Walled Carbon Nanotubes under Hydrostatic Pressure. *Phys. Rev. Lett.* **85**, 1887-1889 (2000).

23 Lu, J. P. Elastic Properties of Carbon Nanotubes and Nanoropes. *Phys. Rev. Lett.* **79**, 1297-1300 (1997).

24 Salvetat, J.-P. *et al.* Elastic and Shear Moduli of Single-Walled Carbon Nanotube Ropes. *Phys. Rev. Lett.* **82**, 944-947 (1999).